

Human Coronavirus 229E Binds to CD13 in Rafts and Enters the Cell through Caveolae

Ryuji Nomura,^{1*} Asuka Kiyota,² Etsuko Suzaki,² Katsuko Kataoka,² Yoshihide Ohe,³
Kaoru Miyamoto,⁴ Takao Senda,¹ and Toyoshi Fujimoto⁵

Department of Anatomy I, Fujita Health University School of Medicine, Toyoake 470-1192,¹ Department of Histology and Cell Biology, Hiroshima University Graduate School of Biomedical Sciences, Hiroshima 734-8551,² Biosignal Research Center, Institute for Molecular and Cellular Regulation, Gunma University, Maebashi 371-8512,³ Department of Biochemistry, Fukui Medical University, Matsuoka 910-1193,⁴ and Department of Anatomy and Molecular Cell Biology, Nagoya University Graduate School of Medicine, Nagoya 466-8550,⁵ Japan

Received 14 May 2003/Accepted 11 May 2004

CD13, a receptor for human coronavirus 229E (HCoV-229E), was identified as a major component of the Triton X-100-resistant membrane microdomain in human fibroblasts. The incubation of living fibroblasts with an anti-CD13 antibody on ice gave punctate labeling that was evenly distributed on the cell surface, but raising the temperature to 37°C before fixation caused aggregation of the labeling. The aggregated labeling of CD13 colocalized with caveolin-1 in most cells. The HCoV-229E virus particle showed a binding and redistribution pattern that was similar to that caused by the anti-CD13 antibody: the virus bound to the cell evenly when incubated on ice but became colocalized with caveolin-1 at 37°C; importantly, the virus also caused sequestration of CD13 to the caveolin-1-positive area. Electron microscopy confirmed that HCoV-229E was localized near or at the orifice of caveolae after incubation at 37°C. The depletion of plasmalemmal cholesterol with methyl β -cyclodextrin significantly reduced the HCoV-229E redistribution and subsequent infection. A caveolin-1 knockdown by RNA interference also reduced the HCoV-229E infection considerably. The results indicate that HCoV-229E first binds to CD13 in the Triton X-100-resistant microdomain, then clusters CD13 by cross-linking, and thereby reaches the caveolar region before entering cells.

Recent studies have revealed that the plasma membranes of cells contain microdomains with discrete molecular compositions. Rafts are sphingolipid- and cholesterol-rich membrane microdomains that are thought of as platforms for signal transduction (39, 40). Although there are still many controversies regarding how rafts exist in living cells, it is generally agreed that cholesterol is indispensable for their integrity and that the detergent-resistant membrane (DRM) fraction is the *in vitro* correlate of the raft. Because acyl chains of sphingolipids and glycosylphosphatidylinositol (GPI)-anchored proteins enriched in the DRM fraction are more highly saturated than those of glycerolipids in the bulk membrane, the raft domain is thought to show less fluidity than nonraft areas of the plasma membrane. However, it is difficult to capture rafts morphologically because their shape and size are likely to change dynamically (40).

On the other hand, caveolae were first defined morphologically as invaginations of the plasma membrane (49). They are also susceptible to cholesterol depletion (31). Moreover, caveolin-1, -2, and -3, which were identified as major components of caveolae (31, 35, 44, 47), are highly enriched in the DRM fraction (2, 12, 14, 36). Several results suggest that many molecules are shared by rafts and caveolae but that at least several molecules that are enriched in the DRM fraction are not concentrated in caveolae (11). Thus, caveolae are not sim-

ply a stabilized form of rafts, but there should be a regulatory mechanism (as yet unknown) to control the molecular distribution between caveolae and rafts.

It has been shown that cross-linked raft molecules, such as GPI-anchored proteins, glycolipids, sphingomyelin, and cholesterol, are sequestered to caveolae (13, 25). The underlying mechanism is not clearly defined, but the cross-linking may combine unstable small rafts and give rise to stable large rafts (4); the latter may somehow become hooked to caveolae. The phenomenon is an indication of the close relationship between rafts and caveolae, but its physiological and pathological relevance has not been clear.

In searching for a new molecule that is enriched in the DRM fraction, we found that CD13, or aminopeptidase N, is its predominant component in human fibroblasts. CD13 has been known to be a receptor for human coronavirus 229E (HCoV-229E) (50). Considering the behavior of cross-linked raft molecules as described above, we assumed that the HCoV-229E particle could work as a polyvalent ligand and cause a similar redistribution of CD13 as that induced by anti-CD13 antibodies. In the present study, we indeed observed that the virus particle, initially binding to the cell surface apparently in a random fashion, became aggregated to caveolae in a cholesterol-dependent manner. Furthermore, cholesterol depletion as well as caveolin-1 knockdown inhibited virus entry into the cells. The results indicate that the integrity of the sphingolipid- and cholesterol-rich microdomain is indispensable for infection by HCoV-229E and suggest that manipulation of the membrane lipids could be used as a preventive measure.

* Corresponding author. Mailing address: Department of Anatomy I, Fujita Health University School of Medicine, Toyoake, Aichi 470-1192, Japan. Phone: 81-562-93-2648. Fax: 81-562-93-5904. E-mail: rnomura@fujita-hu.ac.jp.

MATERIALS AND METHODS

Cells and virus. Human fibroblasts were explanted from biopsied normal human adult skin. A human embryonic lung cell line (L132) and HCoV-229E were kindly donated by Ichiro Matsumoto (Iwate Medical University, Morioka, Japan). The cells were grown in Dulbecco's minimum essential medium (DMEM; Nihonseiyaku, Tokyo, Japan) supplemented with either 10% fetal calf serum (for human fibroblasts) or 10% bovine serum (for L132 cells), 50 U of penicillin/ml, and 0.05 mg of streptomycin/ml at 37°C.

For preparation of a virus solution, L132 cells were incubated with HCoV-229E for 1 h at 33°C and cultured at the same temperature for 2 days. The total solution was subjected to three cycles of freezing-thawing, and the supernatant was stored at -80°C. The virus solution was concentrated by the method used for *Mouse hepatitis virus*, a member of the *Coronaviridae* (43).

Antibodies. A rabbit anti-HCoV-229E antiserum (24) was also provided by Ichiro Matsumoto. A mouse anti-coronavirus antibody (Chemicon International, Inc., Temecula, Calif.), mouse anti-caveolin-1 antibody (clones 2234 and 2297; Transduction Laboratories, Lexington, Ky.), rabbit anti-caveolin-1 antibody (Santa Cruz Biotechnology, Santa Cruz, Calif.), mouse anti-CD13 antibody (clone CLB-mon-gran/2, Q20; Research Diagnostics Inc., Flanders, N.J.), rabbit anti-CD13 antibody (Santa Cruz Biotechnology), mouse anti-human transferrin receptor (TfR, or CD71) antibody (clone RVS-10; Cymbus Biotechnology Ltd., Hants, United Kingdom), rabbit anti-CD71 antibody (Santa Cruz Biotechnology), fluorescein isothiocyanate- and rhodamine-conjugated anti-rabbit immunoglobulin G (IgG) and anti-mouse IgG antibodies (Jackson ImmunoResearch Laboratories, West Grove, Pa.), Alexa 488- and Alexa 568-conjugated anti-rabbit IgG and anti-mouse IgG antibodies (Molecular Probes, Inc., Eugene, Oreg.), and horseradish peroxidase-conjugated anti-rabbit IgG and anti-mouse IgG antibodies (Jackson ImmunoResearch Laboratories) were purchased. The specificities of the anti-HCoV-229E and anti-CD13 antibodies were confirmed by Western blotting and immunoprecipitation (data not shown).

Isolation of DRMs and peptide sequencing. Isolation of the DRM fraction was performed by the method of Hope and Pike (18), with minor modifications. Human fibroblasts were treated with 1% Triton X-100 in TNE (25 mM Tris, 150 mM NaCl, 5 mM EDTA, 1 mM phenylmethylsulfonyl fluoride, pH 7.5) for 20 min on ice and centrifuged at 200,000 × g for 1 h at 4°C. The pellet was suspended in 1% Triton X-100 in TNE and homogenized with a Dounce homogenizer. The solution was centrifuged, suspended again in 1% Triton X-100 in TNE, and mixed with an equal volume of 80% sucrose in TNE. The mixture was overlaid with 38% sucrose in TNE and 5% sucrose in TNE and centrifuged at 270,000 × g for 15 to 20 h at 4°C. A light-scattering band seen at the boundary between the 38 and 5% sucrose solutions was diluted four- to fivefold with TNE and centrifuged at 200,000 × g for 1 h at 4°C. The pellet was dissolved, separated by sodium dodecyl sulfate-polyacrylamide gel electrophoresis (SDS-PAGE) with a 5% acrylamide gel, and electrotransferred to a polyvinylidene difluoride membrane. A 160-kDa band was digested with lysyl endopeptidase and subjected to amino acid sequencing. To assess the enrichment of CD13 in the DRM, we subjected the total cell lysate in 1% Triton X-100-TNE to sucrose density gradient ultracentrifugation and took six fractions by puncturing the bottom of the tube. The proteins were precipitated in cold acetone, dissolved in SDS sample buffer, and analyzed by Western blotting.

Immunofluorescence microscopy. To observe the localization of CD13 and TfR, we treated human fibroblasts cultured on glass coverslips on ice with an anti-CD13 or anti-TfR antibody for 30 min and then with a fluorochrome-conjugated secondary antibody for 30 min, rinsed the cells, and incubated them for 0 to 60 min at 37°C. After being fixed with 3% formaldehyde in 0.1 M sodium phosphate buffer for 10 min, the cells were permeabilized with 0.1% Triton X-100 for 5 min, treated with 3% bovine serum albumin for 10 min, and labeled for caveolin-1.

To keep track of HCoV-229E, we allowed human fibroblasts to bind to HCoV-229E on ice, rinsed the cells, and incubated them for 0 to 3 h at 37°C. The cells were fixed and treated in the same manner as described above and were doubly labeled for HCoV-229E or CD13 in combination with caveolin-1. To quantify the degree of colocalization, we took images of 20 cells with a Zeiss LSM510 laser confocal scanning microscope under the same conditions. The colocalization ratio was obtained by dividing the number of pixels with signals for both caveolin-1 and HCoV-229E above a certain threshold level by the number of pixels with an HCoV-229E signal. The experiment was performed three times and representative results are shown below.

For some experiments, to examine the influence of cholesterol depletion, we treated cells with 2 mM methyl β-cyclodextrin (MβCD; Sigma Chemical Co., St. Louis, Mo.) in DMEM for 30 min at 37°C before incubating them with HCoV-229E. To exclude the possibility of irreversible damage caused by the above

treatment, we further incubated some cells with an MβCD-cholesterol complex for 30 min at 37°C to replenish cholesterol. MβCD-cholesterol was prepared as described previously (16); briefly, cholesterol in methanol-chloroform (1:1) was dried and suspended in MβCD in DMEM-0.1× phosphate-buffered saline. The solution was sonicated and rotated at 37°C overnight. After the pH was adjusted to 7.4, the mixture was filtered and diluted with DMEM. The final concentrations were about 1 mM MβCD and 100 μg of cholesterol/ml.

Western blotting. Total cell lysates and fractions from sucrose density gradient ultracentrifugation were solubilized in SDS sample buffer, electrophoresed in 11% acrylamide gels, and transferred to polyvinylidene difluoride membranes. The blots were incubated with primary antibodies followed by a horseradish peroxidase-conjugated secondary antibody, and the reaction was visualized with SuperSignal West Dura Extended Duration substrate (Pierce, Rockford, Ill.).

Electron microscopy. Human fibroblasts were incubated with HCoV-229E for 60 min on ice, rinsed, and kept at 37°C for 0 to 3 h. The cells were fixed with 2.5% glutaraldehyde in 0.1 M sodium phosphate buffer for 30 min on ice, incubated with osmium tetroxide, stained en bloc with uranyl acetate, and embedded in Quetol 812. Ultrathin sections were counterstained with uranyl acetate and lead citrate. To quantify the accumulation of HCoV-229E in caveolae, we measured the proportion of HCoV-229E localized within 150 nm of the orifices of caveolae by using printed electron micrographs.

Reverse transcriptase PCR (RT-PCR). Human fibroblasts bound to HCoV-229E were treated with 0.25% trypsin and 0.02% EDTA in PBS to remove viruses adhering to the cell surface, and the total RNA was extracted by the use of MagExtractor-RNA (Toyobo Co., Ltd., Osaka, Japan). The total RNA was reverse transcribed with ReverTra Ace (Toyobo Co., Ltd.) and an oligo(dT)₂₀ primer and was amplified with the following primer sets: 5'-ATGTTCTCTAA GCTAGTGGATGA-3' and 5'-TTAGAAATCAATAACTCGTTTAG-3' for the E-protein coding region of HCoV-229E RNA and 5'-ACCACAGTCCATG CCATCAC-3' and 5'-TCCACCACCCTGTTGCTGTA-3' for glyceraldehyde-3-phosphate dehydrogenase (G3PDH) mRNA. To estimate the extent of intracellular entry of HCoV-229E, we performed PCRs with 32 and 35 amplification cycles for the HCoV-229E E protein and with 22 and 25 cycles for G3PDH.

Knockdown of caveolin-1 by RNA interference. A double-stranded small interfering RNA (siRNA) designed to target the human caveolin-1 mRNA (14) was purchased from Dharmacon Research (Lafayette, Colo.). A control IX siRNA (Dharmacon Research) was used as a control. Human fibroblasts were transfected with annealed siRNAs by the use of Oligofectamine (Invitrogen, Carlsbad, Calif.) and were subcultured 24 h later. Forty-eight hours after being subcultured, the cells were bound with HCoV-229E on ice, rinsed, and incubated for another 48 h at 37°C. The cells were either fixed for immunofluorescence microscopy or processed for Western blotting, and the effect of the caveolin-1 knockdown on the expression of the coronavirus N protein was estimated. To measure the proportion of cells expressing the N protein by microscopy, we incorporated 10 random fields obtained by laser confocal scanning microscopy. The experiment was performed three times.

RESULTS

Identification of CD13 in DRM of human fibroblasts. Human fibroblasts were treated with 1% Triton X-100 in TNE on ice and then subjected to sucrose density gradient ultracentrifugation. Triton X-100-insoluble material floating at the boundary of the 5 and 38% sucrose solutions was recovered and analyzed by SDS-PAGE. Silver staining visualized 18 bands (Fig. 1A). A prominent band at 160 kDa was identified as CD13 by amino acid sequencing of two peptides and by database searching (FASTA; Genome Net [http://fasta.genome.ad.jp/]) (Fig. 1A). To examine the extent of CD13 enrichment in the DRM, we analyzed the fractions obtained by sucrose density gradient ultracentrifugation by Western blotting (Fig. 1B). CD13 as well as caveolin-1 was enriched in the DRM fraction, whereas TfR, a nonraft membrane molecule, and α-tubulin, a cytosolic protein, were recovered in the bottom fraction (Fig. 1B). This result indicates a marked enrichment of CD13 in the DRM.

Immunofluorescence microscopy of CD13. When living human fibroblasts were incubated with an anti-CD13 antibody

of cells exhibiting extensive colocalization of HCoV-229E and caveolin-1 was 6.4%. When cells bound with HCoV-229E were incubated for 1 h at 37°C, the frequency of colocalization of HCoV-229E and caveolin-1 increased markedly (Fig. 3d to f); although less conspicuous than CD13 cross-linked by antibodies, HCoV-229E also showed a linear alignment (Fig. 3d). After 3 h of incubation at 37°C, the proportion of cells showing colocalization of HCoV-229E and caveolin-1 was 31.2% (Fig. 3g to l).

We also examined the behavior of CD13 when cells were bound with HCoV-229E. When cells were incubated with HCoV-229E on ice and fixed without warming, labeling of CD13 was observed evenly on the cell surfaces (Fig. 3m to o). Binding of HCoV-229E and incubation at 37°C caused clustering of CD13 and its colocalization with caveolin-1. These results indicate that CD13 bound by HCoV-229E behaves in the same manner as that cross-linked with the anti-CD13 antibody (Fig. 3p to r).

Electron microscopy of HCoV-229E redistribution. We examined the distribution of HCoV-229E particles by electron microscopy. When cells were incubated with HCoV-229E on ice and fixed without warming, most viruses were found in the flat portion of the plasma membrane (Fig. 4A, panels a and b); the proportion of HCoV-229E particles that were associated with caveolae was 2.2% (Fig. 4B). For the present study, caveolae were defined morphologically as noncoated plasmalemmal invaginations of 50 to 80 nm in diameter. A small number of noncoated, noncaveolar invaginations could exist, but we previously observed that most noncoated invaginations in human fibroblasts are labeled by an anti-caveolin-1 antibody (T. Fujimoto and R. Nomura, unpublished observation). After 3 h of incubation at 37°C, the number of viruses associated with caveolae increased (Fig. 4A, panels c to f), to a proportion of 29.4% (Fig. 4B). The increase in the number of viruses associated with caveolae was statistically significant (chi-square test for independence; $P < 0.0001$). In contrast, clathrin-coated pits were never observed in the vicinity of the virus particles (Fig. 4A, panel g). Even after 3 h, however, no virus particles were observed in the lumens of caveolae. Notably, cross-bridge structures of high electron density were frequently observed between virus particles and the plasma membrane (Fig. 4A, panel a and inset of panel b).

Inhibition of HCoV-229E redistribution and intracellular entry by cholesterol depletion. The integrity of the sphingolipid- and cholesterol-rich microdomain is known to depend on cholesterol. To examine whether the behavior of HCoV-229E changes when plasmalemmal cholesterol is depleted, we treated cells with M β CD before allowing them to bind with HCoV-229E. According to a Western blot analysis, the amount of HCoV-229E N protein, representing the number of virus particles bound to the cell surface, did not change upon cholesterol depletion (Fig. 5A); the replenishment of cholesterol by M β CD-cholesterol also did not affect the amount of HCoV-229E N protein. Furthermore, either depletion or replenishment of cholesterol did not change the extent of colocalization of HCoV-229E and caveolin-1 when cells were incubated with the virus on ice (5.3 to 7.8%) (Fig. 5B). After incubation at 37°C for 3 h, the colocalization ratio became 23.8% in the control, whereas the ratio (6.3%) was significantly lower in cells that were depleted of cholesterol by M β CD (Fig.

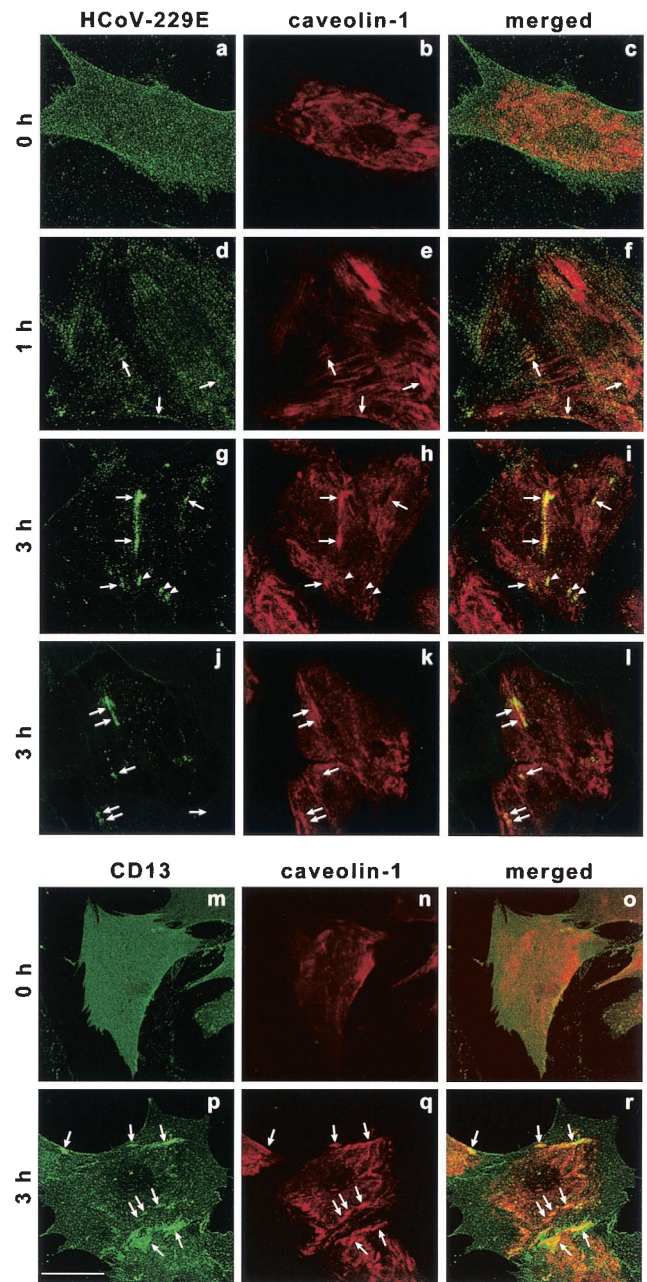


FIG. 3. Immunofluorescence microscopy of human fibroblasts bound to HCoV-229E. Optical sections obtained by laser confocal scanning microscopy were stacked. The cells were treated with HCoV-229E on ice and incubated at 37°C for 0 h (a to c and m to o), 1 h (d to f), or 3 h (g to l and p to r). After fixation, the cells were labeled with an anti-HCoV-229E or anti-CD13 antibody in combination with an anti-caveolin-1 antibody. Labeling for caveolin-1 was always seen as patches (b, e, h, k, n, and q). Labeling for HCoV-229E was seen as randomly distributed dots in cells kept on ice (a); after 1 h of incubation at 37°C, HCoV-229E showed some linear alignment, and colocalization of HCoV-229E and caveolin-1 was seen occasionally (d to f; arrows); and after 3 h at 37°C, the colocalization of HCoV-229E and caveolin-1 became prominent (g to l; arrows). The colocalization of HCoV-229E and caveolin-1 in small clusters was often observed (g to i; arrowheads). Labeling for CD13 was seen as randomly distributed dots at 0 h (m) but showed extensive colocalization with caveolin-1 after 3 h of incubation at 37°C (p to r; arrows). Bar = 50 μ m.

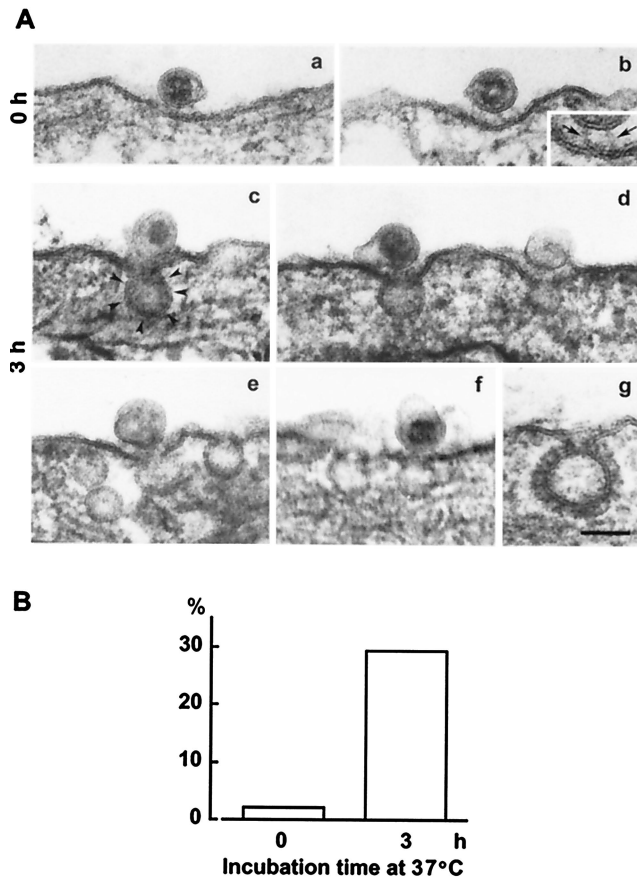


FIG. 4. Electron microscopy of human fibroblasts bound to HCoV-229E. (A) The cells were treated with HCoV-229E on ice and incubated at 37°C for 0 h (a and b) or 3 h (c to g) before fixation. At 0 h, most viruses bound to the flat portion of the plasma membrane (a and b). After 3 h of incubation at 37°C, viruses localized at or within 150 nm of the orifices of caveolae (c to f) were observed frequently. In contrast, clathrin-coated pits (g) were not observed near the virus particles. Cross-bridge structures of high electron density were observed between the virus particles and the plasma membrane (a, inset of b [arrows]). Caveolae are shown by arrowheads (c). Bar = 100 nm. (B) Quantification of HCoV-229E associated with caveolae. The proportion of HCoV-229E localized at or within 150 nm of the orifices of caveolae was calculated by the use of electron micrographs. The proportion increased significantly by 3 h of incubation at 37°C (29.4 versus 2.2%) (chi-square test for independence; $P < 0.0001$).

5B) (Mann-Whitney U test; $P < 0.0001$). The ratio was recovered to 22.4% when cholesterol was replenished, inferring that the M β CD treatment did not affect the cell function irreversibly.

The effect of cholesterol depletion on the intracellular entry of HCoV-229E was also examined. After the virus particles adhering to the cell surface were removed by trypsin, the total RNAs were extracted and the genomic RNA of HCoV-229E was analyzed by RT-PCR. Immediately after incubation with the virus on ice, the RT-PCR products for the control, cholesterol-depleted, and cholesterol-depleted and -replenished samples were equivalent in intensity. This result shows that the amount of HCoV-229E bound to the cell surface was not affected by the manipulation of cholesterol (Fig. 6, lanes 2 to 4). Trypsinization drastically decreased the amount of RT-PCR product in all samples (Fig. 6, lanes 5 to 7), which indicates that virus particles

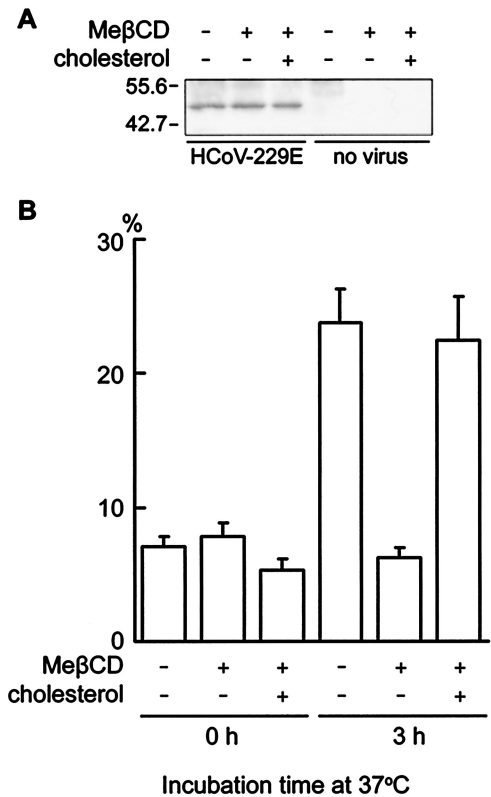


FIG. 5. Effect of M β CD on binding and redistribution of HCoV-229E. The cells were bound to HCoV-229E on ice after being preincubated with nothing, with M β CD alone, or sequentially with M β CD and then an M β CD-cholesterol complex (cholesterol). (A) Western blot analysis with anti-HCoV-229E antiserum. Fifty-kilodalton bands were observed in all samples of cells bound to HCoV-229E (lanes 1 to 3) but were not detected without the virus treatment (lanes 4 to 6). (B) Degree of colocalization of HCoV-229E and caveolin-1. The ratio of colocalization after 3 h of incubation at 37°C was 23.8% for the control, whereas it was significantly lower for cells treated with M β CD (6.3%). The ratio recovered to the control level when cells treated with M β CD were replenished with cholesterol by the addition of an M β CD-cholesterol complex (22.4%) (Mann-Whitney U test; $P < 0.0001$). The results are representative of three experiments.

hardly entered the cell when they were kept on ice. In contrast, after incubation at 37°C for 3.5 h, a significant amount of HCoV-229E RNA was detected in the control sample even after trypsinization. The amount decreased significantly in the cholesterol-depleted cells but was recovered to the control level in the cholesterol-depleted and -replenished cells (Fig. 6, lanes 8 to 10). These results demonstrate that cholesterol depletion inhibits the intracellular entry of HCoV-229E.

Inhibition of HCoV-229E intracellular entry by caveolin-1 knockdown. To examine whether caveolin-1 plays a critical role in virus entry, we tested the effect of a caveolin-1 knockdown on HCoV-229E infection. According to a Western blot analysis, the amount of HCoV-229E N protein, representing the number of virus particles bound to the cell surface, did not change after transfection with a control siRNA or caveolin-1 siRNA (Fig. 7A), but the amount of caveolin-1 decreased after treatment with the caveolin-1 siRNA in a dose-dependent manner (Fig. 7A and B, panel e). When the cells were incubated at 37°C for 48 h after virus binding, labeling for HCoV-

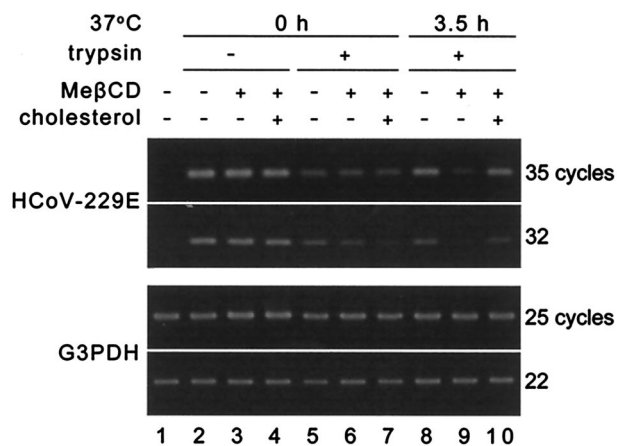


FIG. 6. Effect of M β CD on intracellular entry of HCoV-229E. The data shown are from RT-PCRs of HCoV-229E RNA and G3PDH mRNA. The amount of the PCR template was normalized by using G3PDH in two different PCR cycles. The cells were incubated in the presence (+) or absence (-) of M β CD and M β CD-cholesterol (cholesterol) before being bound to HCoV-229E on ice and then incubated for 0 or 3.5 h at 37°C. Trypsinization was done to remove virus particles bound to the cell surface for an estimation of the virus amount that entered the cell. Without the virus treatment, HCoV-229E RNA was not detected (lane 1). For cells kept on ice, the amounts of HCoV-229E RNA were equivalent in all samples, but trypsinization decreased the amount greatly (lanes 2 to 4, no trypsinization; lanes 5 to 7, after trypsinization). After incubation at 37°C for 3.5 h, the intensity of the band was significantly lower for M β CD-treated cells than for control cells or cells that were treated sequentially with M β CD and M β CD-cholesterol (lanes 8 to 10).

229E was observed in the cytoplasm in most control cells, which were either nontransfected or transfected with a control siRNA (Fig. 7B, panels a to c). In contrast, the proportion of cells showing cytoplasmic labeling for HCoV-229E decreased after transfection with the caveolin-1 siRNA, as follows (Fig. 7B, panels d to f): the proportions were 52.0, 42.8, and 40.1% with 5, 20, and 80 nM caveolin-1 siRNA, respectively, which were significantly smaller than that of nontransfected cells (72.2%) or cells transfected with a control siRNA (73.0%) (chi-square test for independence; $P < 0.0001$) (Fig. 7C).

DISCUSSION

CD13 is a type II transmembrane protein, having a short cytoplasmic NH₂-terminal segment and a long extracellular COOH-terminal segment, and exists as a homodimer on the cell surface (30). CD13 is identical to aminopeptidase N (22) and is thought to be engaged in digesting luminal peptides in the small intestine and the renal proximal tubule (37). In relation to viruses, CD13 is known to be a receptor of HCoV-229E (50), porcine coronavirus transmissible gastroenteritis virus (TGEV) (7), and feline and canine coronaviruses (46).

In the present study, we identified CD13 as a major component of DRMs isolated from human fibroblasts. For several cell types, CD13 has been reported to be a component of DRMs (6, 29, 33). As already observed for other DRM molecules, the antibody to CD13 bound to the cell surface evenly when incubated on ice, but the bound antibodies became sequestered to caveolin-1-positive patches when the temperature

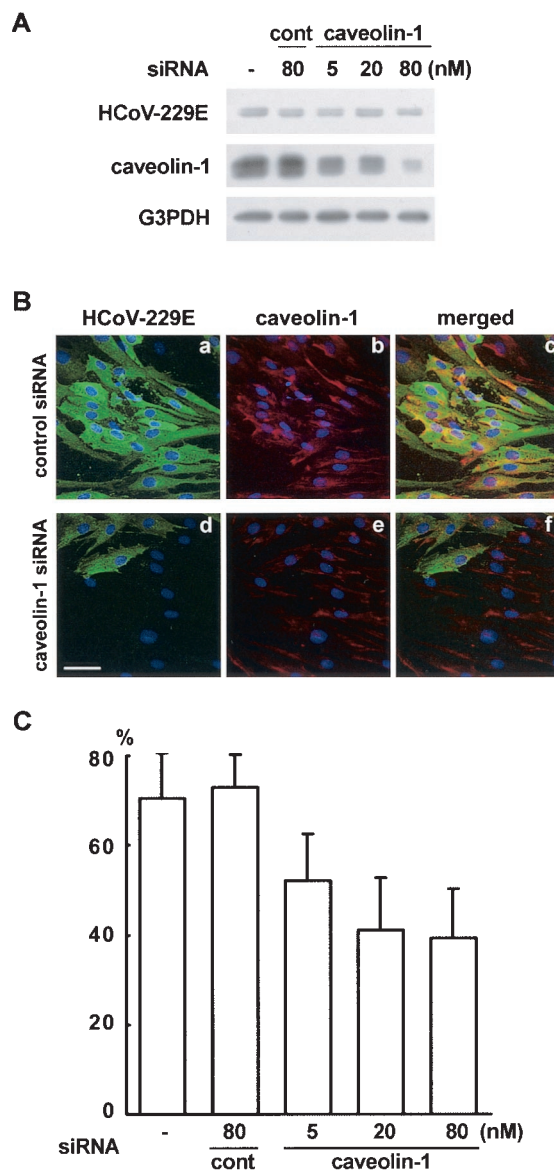


FIG. 7. Effect of caveolin-1 knockdown on binding and intracellular entry of HCoV-229E. The cells were not transfected (-) or were transfected with 80 nM control siRNA (cont) or 5 to 80 nM caveolin-1 siRNA and then were incubated at 37°C for 24 h. Forty-eight hours after subculturing, the cells were bound to HCoV-229E on ice and processed immediately or incubated at 37°C for 48 h. (A) Immunoblotting of total lysates of cells incubated on ice with anti-HCoV-229E, anti-caveolin-1, and anti-G3PDH antibodies. The amounts of the cell lysates were normalized with G3PDH. The amount of caveolin-1 decreased in a dose-dependent manner, and the expression of the HCoV-229E N protein was equivalent in all samples. (B) Immunofluorescence microscopy of cells transfected with 80 nM control siRNA (a to c) and caveolin-1 siRNA (d to f). Cells were bound to HCoV-229E on ice and incubated at 37°C for 48 h. In cells transfected with the caveolin-1 siRNA, labeling for caveolin-1 decreased (e), and the number of cells showing cytoplasmic HCoV-229E labeling was also reduced (d and f). Bar = 50 μ m. (C) Proportion of cells showing cytoplasmic labeling of HCoV-229E. The proportion was significantly lower in cells transfected with 5, 20, or 80 nM caveolin-1 siRNA (52.0, 42.8, and 40.1%, respectively) than in nontransfected cells (72.2%) or cells transfected with a control siRNA (73.0%) (chi-square test for independence; $P < 0.0001$).

was raised to 37°C. Treatment with an anti-DRM molecule antibody alone was not sufficient for the redistribution, and further cross-linking by a secondary antibody was required (13). In contrast, a similar redistribution of HCoV-229E was observed without any further treatment. Because S proteins, a likely ligand for CD13, exist in multiple copies in HCoV-229E, sufficient cross-linking of CD13 is likely to occur by binding of a virus particle. This conjecture is supported by the observation that CD13 became sequestered to caveolin-1-positive patches when it was bound to HCoV-229E. On the other hand, the relatively slow redistribution of HCoV-229E compared to that of the anti-CD13 antibody may reflect differences in the degrees of cross-linking and the sizes of the ligands.

Notably, cross-linked CD13 molecules showed a streaky distribution along longitudinal lines, which were most likely actin stress fibers, before being sequestered to caveolin-1-positive patches. Although the pattern was less conspicuous, HCoV-229E particles also showed a similar distribution. The longitudinal distribution was also reported for cross-linked β 2-microglobulin, which is eventually endocytosed through caveolae (19). In contrast, other molecules destined for caveolae, e.g., GPI-anchored proteins and ganglioside GM1, did not show such a linear alignment (3, 13). CD13 is a transmembrane protein, and β 2-microglobulin binds to major histocompatibility complex class I, which is also a transmembrane protein; on the other hand, GPI-anchored proteins and ganglioside GM1 are confined to the outer leaflet. The cross-linking of CD13 by antibodies may induce binding to actin filaments, either directly or indirectly, and may cause the longitudinal alignment. HCoV-229E may activate the same mechanism by binding to CD13. Further studies will be needed to understand how the actin cytoskeleton is involved in the caveolar sequestration of HCoV-229E.

The colocalization of HCoV-229E and caveolin-1 was decreased significantly by the depletion of cholesterol by a pretreatment with M β CD. Because binding of the virus to the cell was not changed by cholesterol depletion, it was the redistribution process of the virus that was affected by the treatment. Cholesterol depletion by M β CD also decreased the intracellular occurrence of HCoV-229E. These results indicate that the disruption of rafts and caveolae by cholesterol depletion inhibits the virus's redistribution and its subsequent entry into the cell. A redistribution of cross-linked raft molecules to caveolae has been observed repeatedly by the use of antibodies as ligands. We surmise that some viruses, including HCoV-229E, are likely to use the raft-caveola relationship to reach the caveolar region. A recent report that murine hepatitis virus requires membrane cholesterol for cell entry suggests that the same mechanism may be used by other coronaviruses (45).

To examine how caveolae are involved in the intracellular entry of HCoV-229E, we tried to test the effect of a dominant-negative caveolin mutant, DGV-caveolin-3, which was shown to inhibit the entry of simian virus 40 (SV40) and echovirus 1 (23, 32). However, the transfection of any plasmid vector turned out to drastically decrease HCoV-229E binding to the cell surface by an unknown mechanism (data not shown), and this procedure could not be used for our purpose. We thus examined the effect of a caveolin-1 knockdown on HCoV-229E internalization. The binding of the virus to the cell did not change by transfection with a siRNA, and the entry of HCoV-229E was inhibited specifically by the caveolin-1 knockdown.

This result implies that the expression of caveolin-1 is important for infection by HCoV-229E.

Besides SV40 and echovirus 1, various nonenveloped viruses, including mouse polyomavirus and BK polyomavirus, have been reported to enter the cell from caveolae (1, 8, 23, 28, 42). SV40 was shown to be transported to the lumen of the endoplasmic reticulum via an endosome-like compartment named the caveosome (1, 20, 27, 42). However, we could not see HCoV-229E in the caveolar lumen by electron microscopy even at later time points; we also did not see any indication by immunofluorescence microscopy that HCoV-229E was localized to the endosome or the endoplasmic reticulum. This disparity might indicate that although both enveloped and nonenveloped viruses enter cells from caveolae, they may take different routes after leaving the caveolae. In fact, some enveloped viruses belonging to the *Filoviridae*, ranging up to 1,400 nm in length, were reported to enter cells from caveolae (10). Because such large viruses are not likely to be engulfed in caveolae, they might fuse with the caveolar membrane to enter the cytoplasm.

Why are caveolae used as an entry port by HCoV-229E? In the case of SV40, which is incorporated into the caveola-derived caveosome (1, 20, 27, 42), the modification of caveolin may be imperative for the transformation of caveolar invagination. On the other hand, enveloped viruses may not enter the caveolar lumen. For those viruses, the orifice or the neck portion of caveolae rather than the luminal portion may have some property that is appropriate for entry. A unique property of the orifice region was indicated by the preferential formation of a filipin-cholesterol complex when filipin was applied for a short time (38). This result may not indicate a particular enrichment of cholesterol because the filipin-cholesterol complex is formed in other regions of the plasma membrane after a longer incubation (38), but it may reflect some kind of specialization in the caveolar orifice. Further studies are necessary to identify the route of virus entry and to determine how caveolae and caveolin are involved in the process.

TGEV, which also uses CD13 as a receptor, was reported to be endocytosed by clathrin-coated pits in the apical plasma membranes of MDCK cells (17). However, the reported experiments used a canine cell line that overexpressed pig CD13, and the nonphysiological density of the molecule may have affected the results. Moreover, typical caveolar invaginations do not exist in the apical membranes of MDCK cells (34). These differences may be the reasons for the disparity between our result and the cited study.

There are several other viruses that use a receptor that is sequestered to caveolae when it is cross-linked (5, 15, 41, 48). Interestingly, HCoV-OC43, a strain of HCoV belonging to another group, is also one of these viruses (5). Because a coronavirus is the pathogen that causes severe acute respiratory syndrome (9, 11, 21, 26), it is important to examine whether infections by coronaviruses can be prevented by cholesterol depletion. Manipulation of the membrane lipid composition could be both a preventive and a therapeutic measure against many viruses.

ACKNOWLEDGMENTS

We are grateful to Ichiro Matsumoto for L132 cells and HCoV-229E; Shigeko Torihashi, Hiroshi Kogo, Tetsuya Yoshida, Takemasa

Sakaguchi, and Akiko Iizuka-Kogo for helpful discussions and technical advice; and Yukiko Takahashi for excellent technical assistance.

This work was supported by grants-in-aid for scientific research from the Ministry of Education, Culture, Sports, Science, and Technology of the Japanese Government to R.N., E.S., K.K., T.S., and T.F. and by grants to R.N. from the Nissan Science Foundation, the Inamori Foundation, the Hori Information Science Promotion Foundation, the Takeda Science Foundation, and the Uehara Memorial Foundation.

REFERENCES

- Anderson, H. A., Y. Chen, and L. C. Norkin. 1996. Bound simian virus 40 translocates to caveolin-enriched membrane domains, and its entry is inhibited by drugs that selectively disrupt caveolae. *Mol. Biol. Cell* **7**:1825–1834.
- Anderson, R. G. W. 1998. The caveolae membrane system. *Annu. Rev. Biochem.* **67**:199–225.
- Aoki, T., S. Kogure, H. Kogo, M. Hayashi, Y. Ohno-Iwashita, and T. Fujimoto. 2003. Sequestration of cross-linked membrane molecules to caveolae in two different pathways. *Acta Histochem. Cytochem.* **36**:165–171.
- Brown, D. A., and E. London. 1998. Functions of lipid rafts in biological membranes. *Annu. Rev. Cell Dev. Biol.* **14**:111–136.
- Collins, A. R. 1993. HLA class I antigen serves as a receptor for human coronavirus OC43. *Immunol. Investig.* **22**:95–103.
- Danielsen, E. M. 1995. Involvement of detergent-insoluble complexes in the intracellular transport of intestinal brush border enzymes. *Biochemistry* **34**:1596–1605.
- Delmas, B., J. Gelfi, R. L'Haridon, L. K. Vogel, H. Sjoström, O. Noren, and H. Laude. 1992. Aminopeptidase N is a major receptor for the enteropathogenic coronavirus TGEV. *Nature* **357**:417–420.
- Drachenberg, C. B., J. C. Papadimitriou, R. Wali, C. L. Cubitt, and E. Ramos. 2003. BK polyoma virus allograft nephropathy: ultrastructural features from viral cell entry to lysis. *Am. J. Transplant.* **3**:1383–1392.
- Drosten, C., S. Gunther, W. Preiser, S. van der Werf, H. R. Brodt, S. Becker, H. Rabenau, M. Panning, L. Kolesnikova, R. A. Fouchier, A. Berger, A. M. Burguiera, J. Cinatl, M. Eickmann, N. Esciriou, K. Grywna, S. Kramme, J. C. Manuguerra, S. Muller, V. Rieckerts, M. Stürmer, S. Vieth, H. D. Klenk, A. D. Osterhaus, H. Schmitz, and H. W. Doerr. 2003. Identification of a novel coronavirus in patients with severe acute respiratory syndrome. *N. Engl. J. Med.* **348**:1967–1976.
- Empig, C. J., and M. A. Goldsmith. 2002. Association of the caveola vesicular system with cellular entry by filoviruses. *J. Virol.* **76**:5266–5270.
- Fouchier, R. A., T. Kuiken, M. Schutten, G. van Amerongen, G. J. van Doornum, B. G. van den Hoogen, M. Peiris, W. Lim, K. Stöhr, and A. D. Osterhaus. 2003. Aetiology: Koch's postulates fulfilled for SARS virus. *Nature* **423**:240.
- Fra, A. M., E. Williamson, K. Simons, and R. G. Parton. 1994. Detergent-insoluble glycolipid microdomains in lymphocytes in the absence of caveolae. *J. Biol. Chem.* **269**:30745–30748.
- Fujimoto, T. 1996. GPI-anchored proteins, glycosphingolipids, and sphingomyelin are sequestered to caveolae only after crosslinking. *J. Histochem. Cytochem.* **44**:929–941.
- Fujimoto, T., H. Hagiwara, T. Aoki, H. Kogo, and R. Nomura. 1998. Caveolae: from a morphological point of view. *J. Electron Microsc.* **47**:451–460.
- Grundy, J. E., J. A. McKeating, P. J. Ward, A. R. Sanderson, and P. D. Griffiths. 1987. Beta 2 microglobulin enhances the infectivity of cytomegalovirus and when bound to the virus enables class I HLA molecules to be used as a virus receptor. *J. Gen. Virol.* **68**:793–803.
- Han, J., D. P. Hajar, J. M. Tauras, and A. C. Nicholson. 1999. Cellular cholesterol regulates expression of the macrophage type B scavenger receptor, CD36. *J. Lipid Res.* **40**:830–838.
- Hansen, G. H., B. Delmas, L. Besnardeau, L. K. Vogel, H. Laude, H. Sjoström, and O. Noren. 1998. The coronavirus transmissible gastroenteritis virus causes infection after receptor-mediated endocytosis and acid-dependent fusion with an intracellular compartment. *J. Virol.* **72**:527–534.
- Hope, H. R., and L. J. Pike. 1996. Phosphoinositides and phosphoinositide-utilizing enzymes in detergent-insoluble lipid domains. *Mol. Biol. Cell* **7**:843–851.
- Huet, C., J. F. Ash, and S. J. Singer. 1980. The antibody-induced clustering and endocytosis of HLA antigens on cultured human fibroblasts. *Cell* **21**:429–438.
- Kartenbeck, J., H. Stukenbrok, and A. Helenius. 1989. Endocytosis of simian virus 40 into the endoplasmic reticulum. *J. Cell Biol.* **109**:2721–2729.
- Ksiazek, T. G., D. Erdman, C. S. Goldsmith, S. R. Zaki, T. Peret, S. Emery, S. Tong, C. Urbani, J. A. Comer, W. Lim, P. E. Rollin, S. F. Dowell, A. E. Ling, C. D. Humphrey, W. J. Shieh, J. Guarner, C. D. Paddock, P. Rota, B. Fields, J. DeRisi, J. Y. Yang, N. Cox, J. M. Hughes, J. W. LeDuc, W. J. Bellini, and L. J. Anderson. 2003. A novel coronavirus associated with severe acute respiratory syndrome. *N. Engl. J. Med.* **348**:1953–1966.
- Look, A. T., R. A. Ashmun, L. H. Shapiro, and S. C. Peiper. 1989. Human myeloid plasma membrane glycoprotein CD13 (gp150) is identical to aminopeptidase N. *J. Clin. Investig.* **83**:1299–1307.
- Marjomaki, V., V. Pietiäinen, H. Matilainen, P. Upla, J. Ivaska, L. Nissinen, H. Reunanen, P. Huttunen, T. Hyypia, and J. Heino. 2002. Internalization of echovirus 1 in caveolae. *J. Virol.* **76**:1856–1865.
- Matsumoto, I., and R. Kawana. 1992. Virological surveillance of acute respiratory tract illnesses of children in Morioka, Japan. III. Human respiratory coronavirus. *Kansenshogaku Zasshi.* **66**:319–326.
- Mayor, S., K. G. Rothberg, and F. R. Maxfield. 1994. Sequestration of GPI-anchored proteins in caveolae triggered by cross-linking. *Science* **264**:1948–1951.
- Peiris, J. S., S. T. Lai, L. L. Poon, Y. Guan, L. Y. Yam, W. Lim, J. Nicholls, W. K. Yee, W. W. Yan, M. T. Cheung, V. C. Cheng, K. H. Chan, D. N. Tsang, R. W. Yung, T. K. Ng, and K. Y. Yuen. 2003. Coronavirus as a possible cause of severe acute respiratory syndrome. *Lancet* **361**:1319–1325.
- Pelkmans, L., J. Kartenbeck, and A. Helenius. 2001. Caveolar endocytosis of simian virus 40 reveals a new two-step vesicular-transport pathway to the ER. *Nat. Cell Biol.* **3**:473–483.
- Richterova, Z., D. Liebl, M. Horak, Z. Palkova, J. Stokrova, P. Hozak, J. Korb, and J. Forstova. 2001. Caveolae are involved in the trafficking of mouse polyomavirus virions and artificial VPI pseudocapsids toward cell nuclei. *J. Virol.* **75**:10880–10891.
- Riemann, D., G. H. Hansen, L. Niels-Christiansen, E. Thorsen, L. Immerdal, A. N. Santos, A. Kehlen, J. Langner, and E. M. Danielsen. 2001. Caveolae/lipid rafts in fibroblast-like synoviocytes: ectopeptidase-rich membrane microdomains. *Biochem. J.* **354**:47–55.
- Riemann, D., A. Kehlen, and J. Langner. 1999. CD13—not just a marker in leukemia typing. *Immunol. Today* **20**:83–88.
- Rothberg, K. G., J. E. Heuser, W. C. Donzell, Y. S. Ying, J. R. Glenney, and R. G. W. Anderson. 1992. Caveolin, a protein component of caveolae membrane coats. *Cell* **68**:673–682.
- Roy, S., R. Luetterforst, A. Harding, A. Apolloni, M. Etheridge, E. Stang, B. Ralls, J. F. Hancock, and R. G. Parton. 1999. Dominant-negative caveolin inhibits H-Ras function by disrupting cholesterol-rich plasma membrane domains. *Nat. Cell Biol.* **1**:98–105.
- Santos, A. N., J. Langner, M. Herrmann, and D. Riemann. 2000. Aminopeptidase N/CD13 is directly linked to signal transduction pathways in monocytes. *Cell Immunol.* **201**:22–32.
- Scheiffele, P., P. Verkade, A. M. Fra, H. Virta, K. Simons, and E. Ikonen. 1998. Caveolin-1 and -2 in the exocytic pathway of MDCK cells. *J. Cell Biol.* **140**:795–806.
- Scherer, P. E., T. Okamoto, M. Chun, I. Nishimoto, H. F. Lodish, and M. P. Lisanti. 1996. Identification, sequence, and expression of caveolin-2 defines a caveolin gene family. *Proc. Natl. Acad. Sci. USA* **93**:131–135.
- Schnitzer, J. E., D. P. McIntosh, A. M. Dvorak, J. Liu, and P. Oh. 1995. Separation of caveolae from associated microdomains of GPI-anchored proteins. *Science* **269**:1435–1439.
- Semenza, G. 1986. Anchoring and biosynthesis of stalked brush border membrane proteins: glycosidases and peptidases of enterocytes and renal tubuli. *Annu. Rev. Cell Biol.* **2**:255–313.
- Simionescu, N., F. Lupu, and M. Simionescu. 1983. Rings of membrane sterols surround the openings of vesicles and fenestrae, in capillary endothelium. *J. Cell Biol.* **97**:1592–1600.
- Simons, K., and E. Ikonen. 1997. Functional rafts in cell membranes. *Nature* **387**:569–572.
- Simons, K., and D. Toomre. 2000. Lipid rafts and signal transduction. *Nat. Rev. Mol. Cell Biol.* **1**:31–39.
- Soderberg, C., T. D. Giugni, J. A. Zaia, S. Larsson, J. M. Wahlberg, and E. Moller. 1993. CD13 (human aminopeptidase N) mediates human cytomegalovirus infection. *J. Virol.* **67**:6576–6585.
- Stang, E., J. Kartenbeck, and R. G. Parton. 1997. Major histocompatibility complex class I molecules mediate association of SV40 with caveolae. *Mol. Biol. Cell* **8**:47–57.
- Taguchi, F., T. Hayashi, A. Yamada, and K. Fujiwara. 1978. Purification and buoyant density of a mouse hepatitis virus, MHV-S. *Jpn. J. Exp. Med.* **48**:369–371.
- Tang, Z., P. E. Scherer, T. Okamoto, K. Song, C. Chu, D. S. Kohtz, I. Nishimoto, H. F. Lodish, and M. P. Lisanti. 1996. Molecular cloning of caveolin-3, a novel member of the caveolin gene family expressed predominantly in muscle. *J. Biol. Chem.* **271**:2255–2261.
- Thorp, E. B., and T. M. Gallagher. 2004. Requirements for CEACAMs and cholesterol during murine coronavirus cell entry. *J. Virol.* **78**:2682–2692.
- Tresnan, D. B., R. Levis, and K. V. Holmes. 1996. Feline aminopeptidase N serves as a receptor for feline, canine, porcine, and human coronaviruses in serogroup I. *J. Virol.* **70**:8669–8674.
- Way, M., and R. G. Parton. 1995. M-caveolin, a muscle-specific caveolin-related protein. *FEBS Lett.* **376**:108–112.
- Wright, J. F., A. Kurosky, and S. Wasi. 1994. An endothelial cell-surface form of annexin II binds human cytomegalovirus. *Biochem. Biophys. Res. Commun.* **198**:983–989.
- Yamada, E. 1955. The fine structure of the gall bladder epithelium of the mouse. *J. Biophys. Biochem. Cytol.* **1**:445–458.
- Yeager, C. L., R. A. Ashmun, R. K. Williams, C. B. Cardellicchio, L. H. Shapiro, A. T. Look, and K. V. Holmes. 1992. Human aminopeptidase N is a receptor for human coronavirus 229E. *Nature* **357**:420–422.